

ORIGINAL ARTICLE

Fibroblasts drive an immunosuppressive and growth-promoting microenvironment in breast cancer via secretion of Chitinase 3-like 1

N Cohen¹, O Shani¹, Y Raz^{1,2}, Y Sharon¹, D Hoffman¹, L Abramovitz¹ and N Erez¹

Cancer-Associated Fibroblasts (CAFs) are the most prominent stromal cell type in breast tumors. CAFs promote tumor growth and metastasis by multiple mechanisms, including by mediating tumor-promoting inflammation. Immune modulation in the tumor microenvironment plays a central role in determining disease outcome. However, the functional interactions of CAFs with immune cells are largely unknown. Here we report a novel signaling axis between fibroblasts, cancer cells and immune cells in breast tumors that drives an immunosuppressive microenvironment, mediated by CAF-derived Chi3L1. We demonstrate that Chi3L1 is highly upregulated in CAFs isolated from mammary tumors and pulmonary metastases of transgenic mice, and in the stroma of human breast carcinomas. Genetic ablation of Chi3L1 in fibroblasts *in vivo* attenuated tumor growth, macrophage recruitment and reprogramming to an M2-like phenotype, enhanced tumor infiltration by CD8⁺ and CD4⁺ T cells and promoted a Th1 phenotype. These results indicate that CAF-derived Chi3L1 promotes tumor growth and shifts the balance of the immune milieu towards type 2 immunity. Taken together, our findings implicate fibroblast-derived Chi3L1 as a novel key player in the complex reciprocal interactions of stromal cells that facilitate tumor progression and metastasis, and suggest that targeting Chi3L1 may be clinically beneficial in breast cancer.

Oncogene (2017) 36, 4457–4468; doi:10.1038/onc.2017.65; published online 3 April 2017

INTRODUCTION

Breast cancer continues to be one of the leading causes of cancer related mortality in women in the western world, and inflammation is correlated with bad prognosis in breast cancer.¹ Cancer-promoting inflammation is now recognized as a hallmark and an enabling characteristic of cancer.^{2,3} Complex reciprocal interactions between tumor cells and immune cells of both the adaptive and the innate immune systems were shown to play a central role in all stages of tumor growth, metastasis and response to therapy.⁴ Breast tumors exhibit tumor-associated inflammation characterized by infiltration of leukocytes into developing tumors,^{5–7} most abundantly macrophages.⁸ Tumor-associated macrophages (TAMs) were shown to facilitate breast carcinogenesis at all stages,^{8–10} and their abundance in human breast tumors is correlated with worse clinical outcome and with resistance to chemotherapy.^{11,12} The tumor-promoting activities of TAMs include promotion of angiogenesis, tumor invasion and metastasis,^{13,14} and modulating the activity of T cells.^{12,15,16} Macrophages are reprogrammed by signals from cancer cells and from the microenvironment to become tumor-promoting, but the complex interactions between macrophages and fibroblasts in the tumor microenvironment remain largely unresolved.

Cancer-associated fibroblasts (CAFs) are the most prominent stromal cell type in breast carcinomas.¹⁷ CAFs are a vastly heterogeneous multifunctional population of fibroblastic cells shown to promote tumor growth by directly stimulating tumor cell proliferation, by enhancing angiogenesis and by modifying the extracellular matrix (ECM), thus supporting tumor cell invasion.^{18,19} We and others have demonstrated that CAFs also

mediate tumor-promoting inflammation in various murine and human carcinomas, including breast cancer, by secreting cytokines and chemokines that recruit and modulate the function of immune cells in tumors.^{20–25}

Although both CAFs and macrophages are prominent components of the tumor microenvironment that facilitate tumor growth, the functional relationship between these two central cell populations and its correlation with tumor progression in breast cancer is largely unknown. Moreover, many of the factors that mediate the pro-inflammatory and tumor-promoting functions of fibroblasts are still undetermined. Here we show that the glycoprotein Chitinase-3-like-1 (Chi3L1) is secreted by CAFs in breast carcinomas and is a central player in the ability of CAFs to drive a tumor promoting, pro-inflammatory and immunosuppressed microenvironment.

Chi3L1, also known as YKL-40 in humans, is a highly evolutionary conserved secreted protein.²⁶ It contains the conserved chitinase-like enzyme domain but lacks chitinolytic enzymatic activity and is expressed by various cells.²⁶ Chi3L1 was previously implicated in inflammatory disorders, macrophage activation and tumor growth,^{26,27} and shown to be involved in promoting inflammation via regulation of Th2-like immune reactions.²⁸ Chi3L1 is upregulated in a variety of diseases including chronic inflammatory conditions, fibrotic disorders and various types of cancer.^{26,27} Moreover, Chi3L1 was recently shown to have a pro-fibrotic role in idiopathic pulmonary fibrosis.²⁹ We therefore hypothesized that Chi3L1 may play a role in the tumor-promoting activities of CAFs.

¹Department of Pathology, Sackler School of Medicine, Tel Aviv University, Tel Aviv, Israel and ²Department of Obstetrics and Gynecology, Tel Aviv Sourasky Medical Center, Tel Aviv, Israel. Correspondence: Dr N Erez, Department of Pathology, Sackler School of Medicine, Tel Aviv University, Tel Aviv 69978, Israel. E-mail: netaerez@post.tau.ac.il

Received 13 December 2016; revised 2 February 2017; accepted 5 February 2017; published online 3 April 2017

In this study we characterized for the first time the function of CAF-derived Chi3L1. We show that CAF-derived Chi3L1 mediated a novel signaling axis between fibroblasts and immune cells in breast tumors that drives an immunosuppressive, growth-promoting microenvironment. We found that Chi3L1 is highly upregulated in CAFs isolated from mammary tumors and pulmonary metastases in mice, and in the stromal compartment of human breast carcinomas. Chi3L1 enhanced macrophage migration and the expression of an M2-like gene signature. Silencing of Chi3L1 in fibroblasts attenuated tumor growth and macrophage recruitment, augmented infiltration of tumors by CD8⁺ and CD4⁺ T cells and affected the functional differentiation of infiltrating T cells towards a Th1 phenotype.

RESULTS

Chi3L1 is upregulated in CAFs isolated from mammary tumors and lung metastases

Chi3L1 secretion by cancer cells in various solid tumors was shown to be tumor growth-promoting by augmenting the inflammatory response and enhancing angiogenesis.²⁷ Other studies have demonstrated the contribution of Chi3L1 to fibrotic disorders.²⁶ We therefore hypothesized that Chi3L1 may be a mediator of pro-inflammatory and tumor-promoting activities in cancer-associated fibroblasts. To test the expression of Chi3L1 specifically in CAFs during mammary carcinogenesis we isolated fibroblasts directly from fresh tumor tissues of MMTV-PyMT transgenic mice, using our previously described method for isolating fibroblasts by FACS.³⁰ Fibroblasts were isolated from mammary glands of MMTV-PyMT mice at defined tumorigenic stages: early carcinoma-9 weeks, and advanced carcinoma-12 weeks,³¹ or from mammary glands of control non-transgenic littermates. Sorted fibroblasts were analyzed by qRT-PCR for the expression of Chi3L1 (Figure 1a). We found that Chi3L1 was significantly upregulated in CAFs isolated from early or late mammary tumors, as compared with normal mammary fibroblasts (NMFs; Figure 1b). The elevated expression of Chi3L1 in CAFs was also evident at the protein level, analyzed by ELISA of CAF-secreted factors, compared with secreted factors from NMFs (Figure 1c). Since elevated levels of Chi3L1 in the sera of breast cancer patients were correlated with poor prognosis,³² we next analyzed its levels in the peripheral blood of tumor bearing mice (MMTV-PyMT) as compared with normal control mice, and found a striking upregulation of 7-fold in Chi3L1 levels in the serum of mice with mammary tumors (Figure 1d).

To validate our results in human breast cancer, we analyzed Chi3L1 expression in the stromal compartment of human breast tumors compared with normal breast samples, available via the GEO database.³³ Bioinformatics analysis revealed that Chi3L1 is significantly upregulated in the stroma of human breast tumors,

indicating that stromal upregulation of Chi3L1 is operative also in human breast cancer (Figure 1e).

Mortality from breast cancer is almost exclusively a result of metastasis to distant organs. However, very little is known about the role of fibroblasts in facilitating metastatic growth of disseminated tumor cells. To test whether Chi3L1 is upregulated at the metastatic microenvironment, we isolated normal lung fibroblasts (NLFs) or fibroblasts from lungs of end-stage MMTV-PyMT mice bearing spontaneous lung metastases (L-CAFs), and analyzed the expression and secretion of Chi3L1 by qRT-PCR and ELISA, respectively. The presence of metastases was confirmed by gross inspection as well as by qPCR for the PyMT transgene (not shown). Analysis of the results revealed that Chi3L1 was highly upregulated in metastases-associated lung fibroblasts (Figures 1f and g), suggesting that it may play a role in the formation of a permissive metastatic niche in lungs.

Tumor-derived paracrine signaling induces the expression of Chi3L1 in fibroblasts

We previously showed that paracrine signaling by breast cancer cells reprograms fibroblasts to become tumor-promoting and pro-inflammatory.²⁴ In order to test whether the expression of Chi3L1 in mammary fibroblasts is upregulated in response to signaling from tumor cells, we next analyzed the expression of Chi3L1 in fibroblasts following incubation with tumor cell-derived secreted factors. Primary fibroblasts, isolated from normal mammary glands, were incubated with conditioned medium (CM) prepared from the MMTV-PyMT-derived breast carcinoma cell line Met-1.³⁴ Control cells were incubated with serum free medium (SFM). Following incubation, we assessed the expression and secretion of Chi3L1 and found that tumor-derived factors significantly upregulated Chi3L1 in mammary fibroblasts (Figures 1h and i). Notably, Chi3L1 was also induced in NLFs that were incubated with tumor cell CM (Figures 1j and k), suggesting that tumor cells also reprogram stromal cells at the metastatic site.

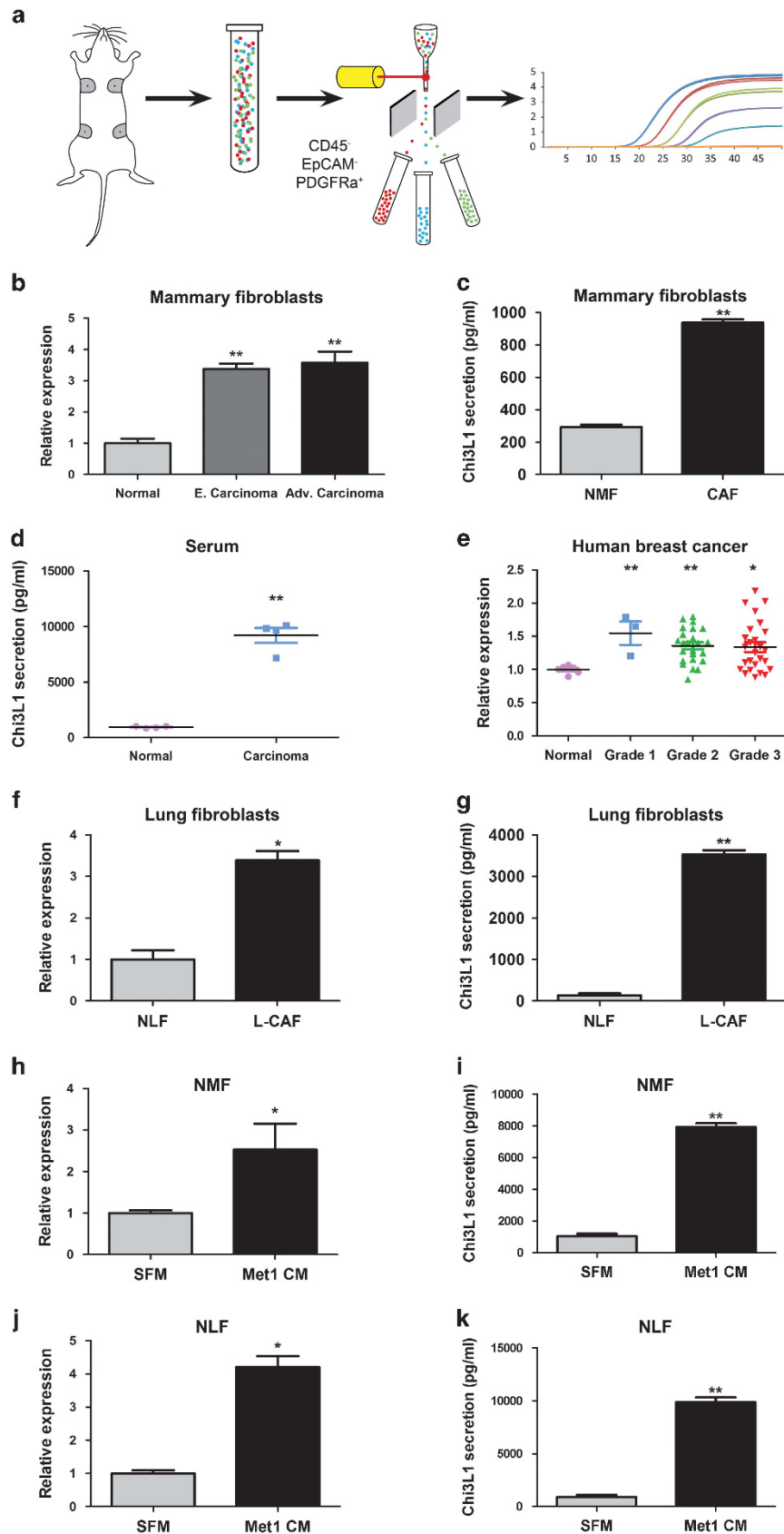
Chi3L1 enhances motility and pro-inflammatory signaling in breast tumor cells

To assess the functional role of Chi3L1 in breast carcinogenesis, we tested the effect of Chi3L1 on tumor cell proliferation and migration, using recombinant Chi3L1 (rChi3L1). Importantly, rChi3L1 concentrations used for these experiments were physiologically relevant, as reflected in Chi3L1 concentrations in fibroblast CM and in mouse serum (Figures 1c and d, respectively). While rChi3L1 did not affect tumor cell proliferation (Supplementary Figure 1), Met-1 mammary carcinoma cells incubated with Chi3L1 exhibited enhanced motility in a scratch closure assay: tumor cells supplemented with Chi3L1 repaired the scratch faster than control cells incubated with SFM (Figures 2a and b).

Figure 1. Chi3L1 is upregulated in CAFs in breast tumors and lung metastases. **(a)** Isolation scheme of CD45⁺ EpCAM⁺ PDGFRα⁺ fibroblasts out of fresh mammary glands by FACS sorting. **(b)** qRT-PCR analysis of Chi3L1 expression in mammary fibroblasts isolated from mammary tissue of age-matched MMTV-PyMT mouse cohorts at distinct stages of tumor progression (normal, early carcinoma, advanced carcinoma). Results are normalized to the housekeeping gene *Gapdh* and to control fibroblasts, isolated from normal mammary glands. Error bars represent s.d. of technical repeats. ***P* < 0.01, *n* = 6, 5, 3 mice in each group, respectively. **(c)** ELISA assay of Chi3L1 secretion from cohorts of NMFs vs CAFs. Error bars represent s.d. of technical repeats. ***P* < 0.01. **(d)** ELISA assay of Chi3L1 in serum of normal mice or end stage MMTV-PyMT mice. Error bars represent s.d. of individual mice. ***P* < 0.01. *n* = 4 mice in each group. **(e)** Chi3L1 expression is upregulated in human breast tumor stroma: expression of Chi3L1 in different tumor grades. Data obtained from the GEO database (GSE9014). Values are presented as relative expression compared to normal breast tissue. **P* < 0.05, ***P* < 0.01. **(f)** qRT-PCR analysis of Chi3L1 expression in lung fibroblasts isolated from cohorts of age-matched normal mice (*n* = 10) or end stage MMTV-PyMT mice (*n* = 6). Results are normalized to the housekeeping gene *Gapdh* and to control fibroblasts. Error bars represent s.d. of technical repeats. **P* < 0.05. **(g)** ELISA assay of Chi3L1 secreted from NLFs vs L-CAFs isolated as in (f). Error bars represent s.d. of technical repeats. ***P* < 0.01. **(h–k)** Tumor-derived paracrine signaling upregulates Chi3L1 in fibroblasts. **(h, j)** qRT-PCR analysis of Chi3L1 expression in pools of NMFs (*n* = 10 mice), or NLFs (*n* = 10 mice) incubated with serum free medium (Control) or with Met-1 CM for 24 h. Results are normalized to the housekeeping gene *Gapdh*. Data presented as fold change from control. **P* < 0.05. **(i, k)** ELISA assay of Chi3L1 secreted from NMFs or NLFs treated as in (h, j). Error bars represent s.d. of technical repeats. ***P* < 0.01.

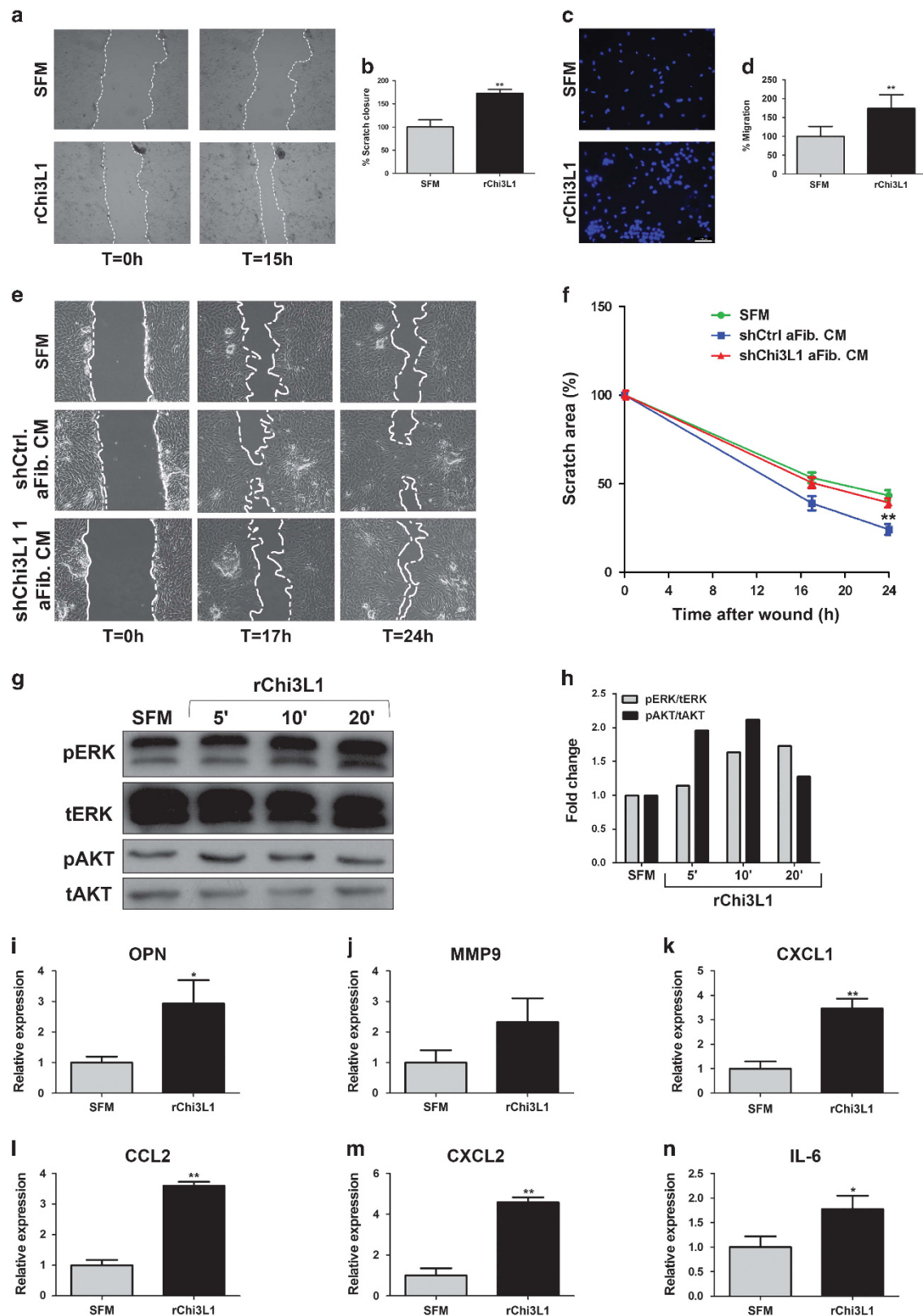
Moreover, incubation of tumor cells with rChi3L1 also enhanced tumor cell migration analyzed by transwell assays. Mammary carcinoma cells incubated with Chi3L1 migrated significantly

better than control cells (Figures 2c and d). To specifically assess the role of fibroblast-derived Chi3L1, we knocked down the expression of Chi3L1 in primary mammary fibroblasts by viral



transduction, utilizing two different shRNAs (shChi3L1 1, 2, Supplementary Figures 2A and B). Control fibroblasts were transduced with scrambled shRNA (shCtrl). Primary mammary fibroblasts were activated with tumor cell-secreted factors to create tumor-activated fibroblasts (aFib), representing CAFs.

Importantly, knockdown of Chi3L1 did not affect the viability, migration and activation of fibroblasts (Supplementary Figures 2C–F). We next incubated tumor cells with conditioned media from shChi3L1 activated fibroblasts and analyzed its effect on tumor cell motility. Analysis of the results revealed that



knockdown of Chi3L1 in fibroblasts significantly attenuated tumor cell motility, compared with tumor cells incubated with control CM or with SFM (Figures 2e and f), indicating that CAF-derived Chi3L1 functionally affects tumor cells. To obtain mechanistic insight we examined which signaling pathways were activated in tumor cells following incubation with Chi3L1. Ectopic expression of Chi3L1 in tumor cells was previously shown to activate the MAPK and PI3K pathways in a cell autonomous manner.^{26,35} We found that Chi3L1 activated these signaling pathways in a paracrine manner: Western blot analysis at different time points following incubation with Chi3L1 indicated that the enhanced motility induced in tumor cells was accompanied by activation of the MAPK and PI3K signaling pathways, quantified by analysis of pERK and pAKT levels (Figures 2g and h). Moreover, since Chi3L1 was reported to promote inflammation,³⁶ we tested its effect on the expression of pro-inflammatory factors by tumor cells. Incubation of breast tumor cells with Chi3L1 resulted in significant upregulation in the expression of pro-inflammatory and pro-invasive factors, including Osteopontin, MMP9, CXCL1, CXCL2, IL-6 and CCL2 (Figures 2i-n). Thus, signaling by Chi3L1 enhances pro-inflammatory gene expression and motility in tumor cells.

Chi3L1 induces angiogenesis and macrophage recruitment *in vivo*
We next analyzed the functional role of Chi3L1 *in vivo*. To that end, we injected female mice subcutaneously with tumor cells in a matrigel plug with or without rChi3L1. Analysis of tissue sections from injected plugs revealed a significant increase in angiogenesis when tumor cells were supplemented with Chi3L1 (Figures 3a and b). Moreover, since we demonstrated *in vitro* that Chi3L1 activated pro-inflammatory signaling in tumor cells, including cytokines that are known to recruit immune cells (for example, CCL2³⁷), we analyzed the tumor plugs for recruitment of macrophages. Analysis of tissue sections from injected plugs revealed that tumor cells injected with Chi3L1 were highly infiltrated by macrophages as compared with control plugs, injected only with tumor cells (Figures 3c and d).

CAF-derived Chi3L1 enhances tumor growth and affects macrophage polarization *in vivo*

Intrigued by these results, we next set out to analyze the functional role of CAF-derived Chi3L1 for tumor growth *in vivo*. To that end, mammary carcinoma cells were admixed with fibroblasts in which the expression of Chi3L1 was knocked down (shChi3L1) and injected orthotopically to mammary glands of FVB/n female mice. Remarkably, silencing of Chi3L1 in fibroblasts significantly inhibited tumor growth and improved the survival of injected mice, although tumor cells also secrete Chi3L1 (Supplementary Figure 3), suggesting that CAF-derived Chi3L1 has a distinct functional role (Figures 3e and f). Moreover, analysis of Chi3L1 in injected tumors revealed significantly lower Chi3L1 expression in tumors injected with shChi3L1-CAFs, suggesting that the absence of Chi3L1 in CAFs may have affected regulatory pathways that reduced the expression of Chi3L1 in tumor cells, and in other cells in the microenvironment. Seeking to elucidate the mechanism by

which CAF-derived Chi3L1 facilitates tumor growth, we analyzed tumor tissue sections by immunostaining and FACS. Analysis of fibroblast activation (α SMA staining) indicated that knockdown of Chi3L1 in fibroblasts was associated with significant reduction in activated α SMA⁺ CAFs in the tumor microenvironment, while collagen deposition (Sirius red staining) was not altered (Figures 3h and i). Interestingly, while rChi3L1 was capable of inducing angiogenesis in the plug assay, angiogenesis was not significantly changed following knockdown of Chi3L1 in CAFs (Figure 3j), suggesting that other CAF-derived factors are operative in the tumor microenvironment. However, in agreement with the plug assay results, tumors in which the expression of Chi3L1 was knocked down in CAFs were significantly less infiltrated with macrophages (Figure 3k). Furthermore, FACS analysis of CD11b⁺F4/80⁺ cells in tumors confirmed that tumors injected with shChi3L1-CAFs contained less macrophages compared with control tumors (Figure 3l), suggesting that CAF-derived signaling is functionally important for macrophage recruitment.

Tumor-associated macrophages (TAMs) are known to be heterogeneous and plastic, and their functional reprogramming is affected by molecular interactions with tumor cells.¹⁴ It is now accepted that the activation status of macrophages is more complex than the dichotomous polarization of M1 and M2, and is better described as a continuum.³⁸ Nevertheless, the activation status of TAMs usually resembles 'M2-like' properties, characterized by promoting tissue repair and remodeling, immune regulation, and tumor promotion.³⁹ In order to test whether CAF-derived Chi3L1 could affect functional reprogramming of macrophages in addition to their recruitment, we analyzed by FACS the ratio of CD206 (an M2 marker) and CD86 (an M1 marker) in TAMs that infiltrated into tumors, and found that tumors injected with shChi3L1-CAFs exhibited a reduction in the M2-like phenotype (Figure 3m). This reduction was evident also in the decreased ratio between the expression of Arginase1 (an M2 marker) and iNOS (associated with M1 macrophages) in tumors in which Chi3L1 was ablated in CAFs (Figure 3n). Thus, CAF-derived Chi3L1 is functionally important for facilitating tumor growth, macrophage recruitment, and affecting macrophage functional activation status.

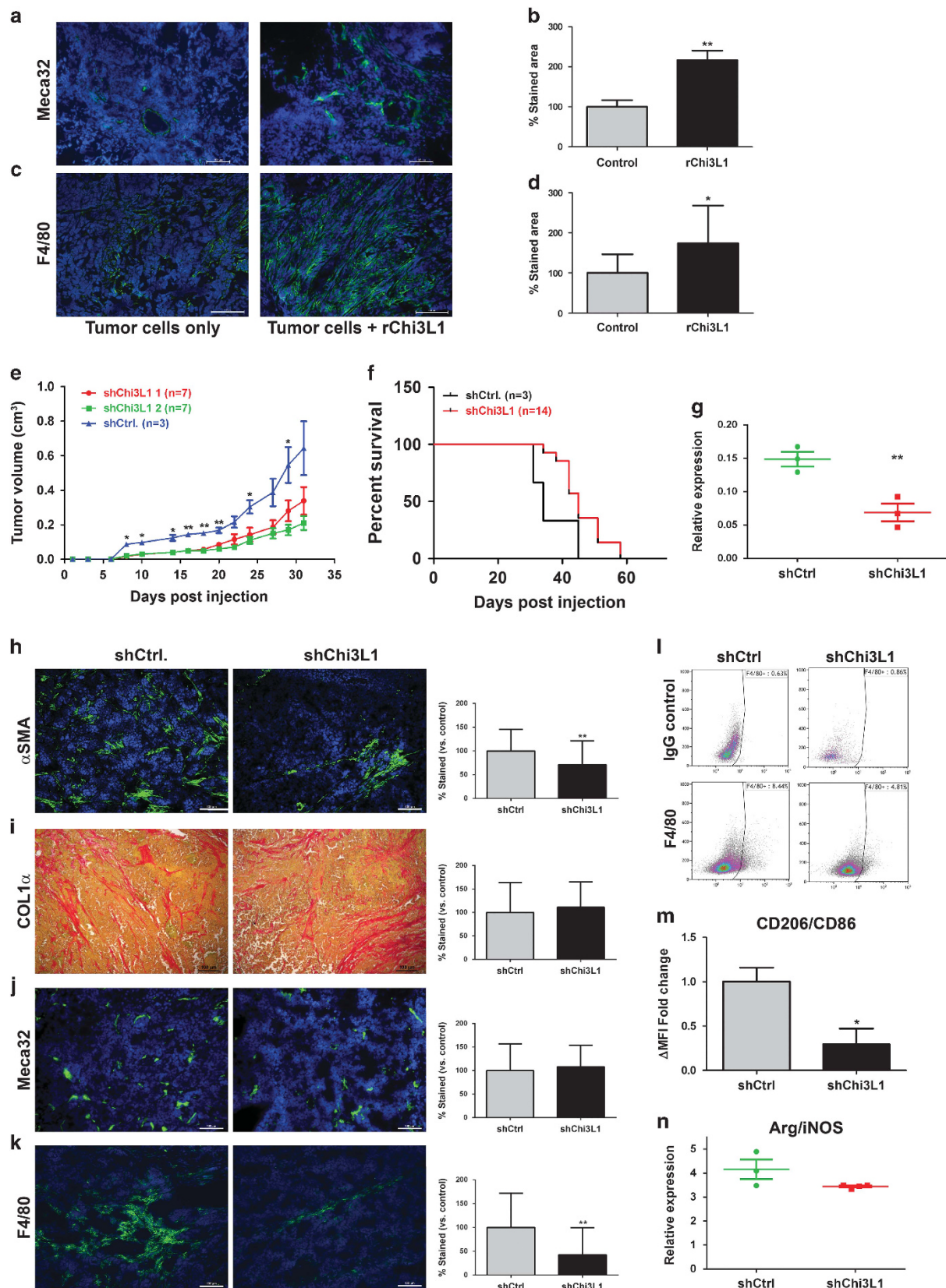
Chi3L1 recruits macrophages and induces an M2-like phenotype
Based on these *in vivo* observations, we next set out to get mechanistic insight on the effect of Chi3L1 on macrophages activation and function. To that end, we analyzed whether Chi3L1 was sufficient to induce macrophage recruitment and M2-like polarization. Cultured macrophages (RAW 264.7) were incubated in SFM or in medium supplemented with rChi3L1 and their migration was analyzed in a transwell assay. Quantification of migrated cells indicated that Chi3L1 markedly enhanced the migration of macrophages (Figures 4a and b). Thus, the pro-inflammatory action of Chi3L1 in tumors likely results from its combined effect on tumor cells, as well as direct recruitment of macrophages. Moreover, Chi3L1 strongly activated the MAPK and

Figure 2. Chi3L1 enhances motility and pro-inflammatory signaling in breast tumor cells. **(a)** Scratch closure assay of Met-1 cells incubated with rChi3L1 or with SFM. **(b)** Quantification of (a). Scratch area was quantified by the ImageJ software. Error bars represent s.d. of 3 fields analyzed from 3 wells each. ****P** < 0.01. Representative of three separate experiments. **(c)** Migration transwell assay of Met-1 mammary tumor cells incubated with serum free medium (Control) or with 100 ng/ml rChi3L1 for 24 h. Representative images of 10 fields analyzed from duplicate wells in three independent experiments. Scale bar = 100 μ m. Magnification X20. **(d)** Quantification of (c). Error bars represent SD. ****P** < 0.01. **(e)** Scratch closure assay of Met-1 cells incubated with CM from shChi3L1 aFib, shCtrl aFib. or SFM. **(f)** Quantification of (e). Scratch area was quantified by the ImageJ software. Error bars represent s.d. of 4 fields analyzed from 2 wells each. ****P** < 0.01. **(g)** Western blot of Met-1 cells incubated with rChi3L1 as indicated. **(h)** Quantification of results shown in (g). Phospho proteins are normalized to total proteins. Data presented as fold change from control. **(i-n)** qRT-PCR analysis of pro-inflammatory genes in Met-1 cells incubated with SFM or with rChi3L1 for 24 h. Results are normalized to the housekeeping gene *Gapdh*. Data presented as fold change from control. Error bars represent s.d. of technical repeats. ***P** < 0.05, ****P** < 0.01. Representative of three separate experiments.

PI3K signaling pathways in macrophages, analyzed by western blot of macrophages (Figures 4c and d).

To further decipher the effect of Chi3L1 on functional activation of primary macrophages, bone marrow (BM)-derived

macrophages were incubated with Chi3L1 and analyzed by qRT-PCR for the expression of genes associated with a pro-tumorigenic 'M2-like' phenotype: Arginase1, CCL17 and YM1, as compared with 'M1-like' associated genes: iNOS, IL-6 and TNF α .⁴⁰ Results



indicated that Chi3L1 reprograms primary macrophages to express M2-related genes, and to down regulate M1-like factors (Figures 4e–j), inducing a significant increase in the ratio of Arginase1/iNOS, typical to the shift from M1 to M2-like macrophage phenotype (Figure 4k). Furthermore, in agreement with the *in vivo* results, incubation of macrophages with Chi3L1 resulted in more than a two-fold increase in the CD206/CD86 ratio, indicating M2-like reprogramming (Figure 4l).

We next verified that mammary CAFs are capable of macrophage reprogramming. To that end, we analyzed the effect of secreted factors from NMFs or from tumor-activated fibroblasts (aFib) on the phenotype of primary macrophages. We found that CAF-derived secreted factors could induce an M2-like phenotype in macrophages, reflected by an increase in the expression of CD206, resulting in a 50% increase in the CD206/CD86 ratio (Supplementary Figure 4). Importantly, knockdown of Chi3L1 expression in mammary fibroblasts by shRNA inhibited CAF-induced M2 reprogramming of macrophages both *in vitro* and *in vivo* (Figures 3l and 4m), indicating that Chi3L1 is a central mediator of CAF-mediated reprogramming of macrophages. Thus, fibroblasts-derived Chi3L1 promotes macrophage recruitment and reprogramming to an M2-like phenotype.

CAF-derived Chi3L1 inhibits T cell infiltration into tumors and drives type 2 inflammation in the tumor microenvironment

TAMs were previously shown to be immunosuppressive and to inhibit T cell-mediated killing of tumor cells by various mechanisms.¹⁴ Importantly, the abundance of CD8⁺ T cells in tumors is associated with better clinical outcome in breast cancer.⁴¹ We therefore analyzed tumors from mice injected with fibroblasts in which Chi3L1 was knocked down (shChi3L1-CAFs) for the presence of T cells. Analysis of tumor tissue by immunostaining and by FACS revealed that tumors in which Chi3L1 was knocked down in CAFs were more infiltrated with T cells as compared with control tumors (Figures 5a, d and e). Specifically, knockdown of Chi3L1 in CAFs resulted in an increase in the abundance of CD8⁺ T cells, indicating that CAF-derived Chi3L1 contributes to the formation of an immunosuppressed microenvironment (Figures 5b, d and e). Interestingly, tumors injected with shChi3L1 CAFs were also more infiltrated with CD4⁺ T cells (Figures 5c–e). To further assess the functional differentiation of the tumor-infiltrating immune milieu, we analyzed the expression of factors known to be associated with Th1 or Th2 subsets in the injected tumors. Analysis of the results revealed that ablation of Chi3L1 in CAFs shifted the balance of type 1 and type 2-related cytokines in the tumor microenvironment towards a Th1 phenotype: while the expression of type 2 inflammation related factors (IL-10, IL-4, Gata3, IL-13) was downregulated or unchanged (Figure 5f and Supplementary Figure 5), the expression of Th1 related factors (IFN γ , TNF- α and Tbet) was upregulated in tumors injected with shChi3L1-CAFs as compared with controls

(Figures 5g–i). These results indicate that CAF-derived Chi3L1 enhances type 2 immunity, either directly, or via its effect on macrophages.

Taken together, our findings establish a novel functional role for CAFs, affecting tumor cells, macrophages and T cells that drives an inflammatory, tumor-promoting, immunosuppressive microenvironment in breast cancer (Figure 5j).

DISCUSSION

The diverse reprogramming of macrophages and T cells was previously shown to affect clinical outcome in breast cancer.^{6,12} In this study, we characterized novel functional interactions between CAFs, cancer cells and immune cells in the microenvironment of breast tumors, mediated by Chi3L1. We show that CAFs mediate immune modulation and functional differentiation of macrophages and T cells in breast cancer and provide mechanistic evidence that this modulation is mediated by their secretion of Chi3L1.

Previous studies have implicated Chi3L1 in multiple malignancies, via its expression in tumor cells and macrophages.^{35,36,42} Elevated levels of Chi3L1 are associated with shorter recurrence-free intervals and with poor prognosis in breast cancer patients.^{32,43,44} Here we show that Chi3L1 is upregulated in mammary CAFs in mice and in the stroma of human breast tumors. CAF-derived Chi3L1 facilitated recruitment of macrophages and affected T cell recruitment and differentiation *in vivo*. Moreover, Chi3L1 could reprogram an M2-like phenotype in macrophages and promote immunosuppression in the tumor microenvironment, as its specific knockdown in fibroblasts resulted in inhibition of tumor growth, prolonged survival, decreased macrophage recruitment and a shift in the infiltrating immune cell milieu towards a less immunosuppressed phenotype.

Ectopic expression of Chi3L1 in tumor cells was previously shown to promote angiogenesis and macrophage recruitment in colon cancer, mediated by autocrine activation of MAPK and JNK signaling.⁴² Here we show that exogenous Chi3L1 activated the MAPK and PI3K signaling pathways in tumor cells and upregulated their motility and expression of pro-inflammatory factors, suggesting that stromal-derived Chi3L1 may affect cancer cells in a paracrine manner within the tumor microenvironment.

The role of fibroblast-derived Chi3L1 was not previously investigated. In this study we demonstrate that Chi3L1 is specifically upregulated in fibroblasts during breast carcinogenesis and lung metastasis. Furthermore, we show that CAF-derived Chi3L1 has a central role in supporting tumor growth *in vivo*: genetic knockdown of Chi3L1 in fibroblasts was sufficient to inhibit tumor growth, despite its continued expression in tumor cells, suggesting that CAF-derived Chi3L1 may have a distinct functional role. These tumor growth-promoting functions could be mediated by the direct effect of CAF-derived Chi3L1 on tumor

Figure 3. Chi3L1 induces angiogenesis and macrophage recruitment *in vivo*. **(a)** Immunofluorescence of Meca-32 in Met-1 matrigel plugs injected with ($n = 4$ mice) or without ($n = 3$ mice) Chi3L1. Representative images out of 45 or 67 fields analyzed in Met-1 only or Met-1+ Chi3L1 injected mice, respectively. Scale bar = 100 μ m. Magnification $\times 20$. **(b)** Quantification of **(a)**. $**P < 0.01$. **(c)** Immunofluorescence of F4/80 in matrigel plugs as in **(a)**. Representative images out of 11 fields analyzed in 3 mice. Scale bar = 100 μ m. Magnification $\times 20$. **(d)** Quantification of **(c)**. $*P < 0.05$. **(e)** Met-1 cells admixed with shChi3L1 fibroblasts or with control fibroblasts (shCtrl) were injected to the right inguinal mammary gland of FVB/n female mice. Error bars represent s.e.m. $*P < 0.05$, $**P < 0.01$. Representative out of three separate experiments performed. **(f)** Survival curve of mice described in **(e)**. $P = 0.0615$. **(g)** qRT-PCR analysis of Chi3L1 expression in mammary tumors injected with shChi3L1 fibroblasts vs shCtrl fibroblasts. Results are normalized to the housekeeping gene *Gapdh*. Error bars represent s.e.m., $**P < 0.01$. $n = 3$ mice per group. **(h–k)** Representative images of α SMA **(h)**, Col1 α **(i)**, Meca32 **(j)** and F4/80 **(k)** staining in tumor sections from mice injected with Met-1 and fibroblasts as indicated. At least 30 fields were analyzed from each group. $n = 6$ (shChi3L1 fibroblasts), $n = 3$ (shCtrl). Scale bar = 100 μ m. Magnification $\times 20$. Quantifications of staining are presented as % from control. $**P < 0.01$. **(l)** FACS analysis of the percentage of F4/80⁺ cells out of CD45⁺CD11b⁺ cells in tumors injected with shChi3L1 fibroblasts vs control. **(m)** CD206/CD86 ratio of Δ MFI values in macrophages isolated from tumors as above. Error bars represent s.e.m. $n = 3$. **(n)** Arginase1/iNOS expression ratio in mammary tumors injected with shChi3L1 fibroblasts vs control. qRT-PCR results were normalized to the housekeeping gene *Gapdh*. Error bars represent s.e.m. $n = 3$ mice per group.

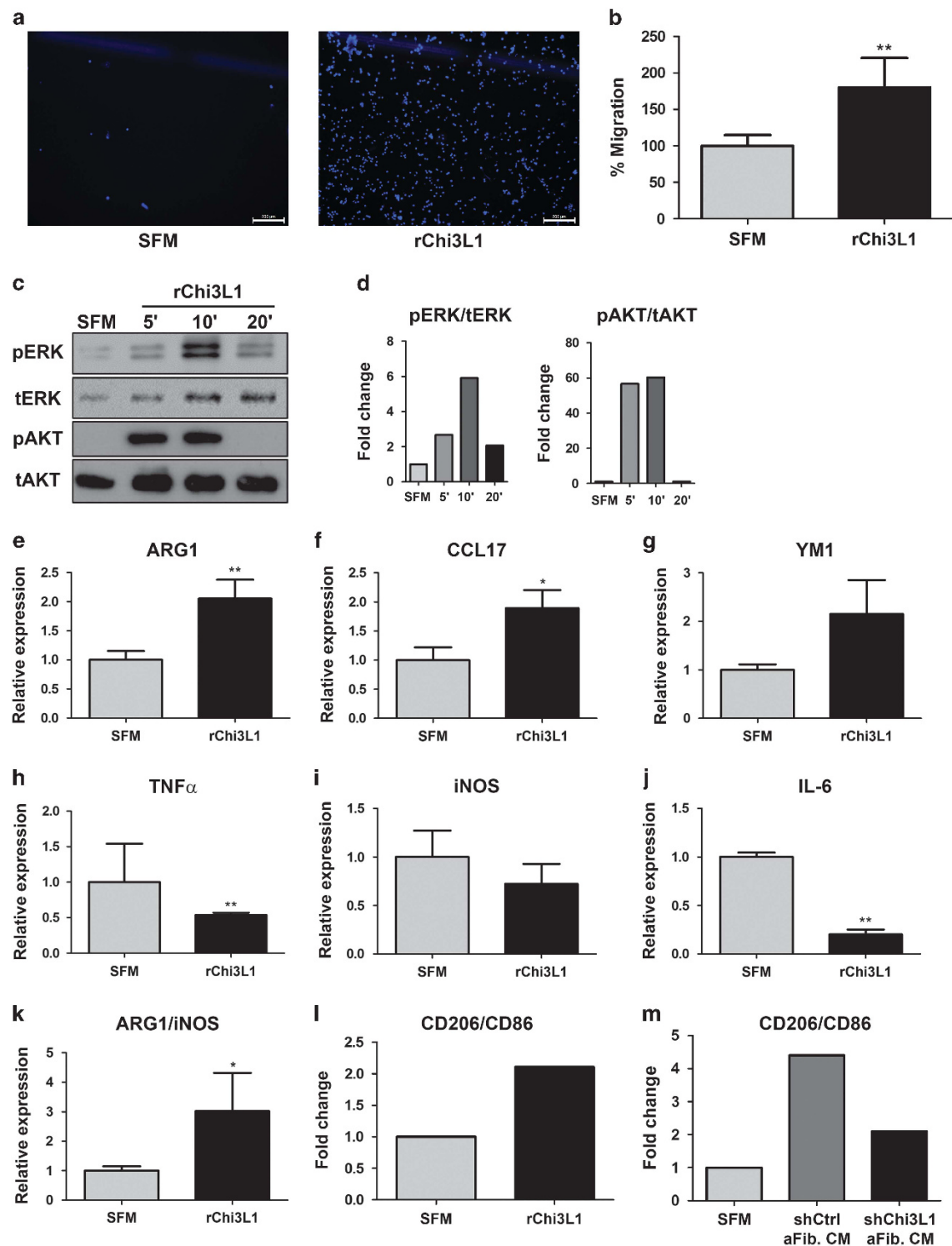


Figure 4. Chi3L1 activates macrophages and induces an M2-like phenotype. **(a)** Migration assay of RAW 264.7 macrophages incubated with SFM or with 100 ng/ml rChi3L1 for 24 h. Representative images out of 13 fields analyzed in duplicate wells. Scale bar = 200 μ m. Magnification $\times 10$. **(b)** Quantification of migration assay in **(a)**. Error bars represent s.d. $**P < 0.01$. Representative of four separate experiments. **(c)** Western blot of RAW 264.7 macrophages incubated with 100 ng/ml rChi3L1 as indicated. **(d)** Quantification of results shown in **(c)**. Phospho-proteins were normalized to total proteins. Data presented as fold change from control. **(e–j)** qRT-PCR expression analysis of M2-related genes **(e–g)** and M1-related genes **(h–j)** in primary BMM incubated with SFM or with Chi3L1 for 24 h. Results are normalized to the housekeeping gene *Gapdh*. Data presented as fold change from control. Error bars represent s.d. of technical repeats. $*P < 0.05$, $**P < 0.01$. Representative of three separate experiments. **(k)** Arginase1/iNOS expression ratio in primary BMM incubated with SFM or with Chi3L1 for 24 h. qRT-PCR analysis results were normalized to the housekeeping gene *Gapdh*. Data presented as fold change from control. Error bars represent s.d. of technical repeats. $*P < 0.05$. Representative of three separate experiments. **(l)** CD206/CD86 ratio in primary BMM incubated with SFM or with Chi3L1 for 24 h, analyzed by FACS. Results were normalized to control. **(m)** CD206/CD86 ratio of BMM incubated with CM from shChi3L1-aFib or from control fibroblasts (shCtrl-aFib), or with SFM. Representative of three separate experiments.

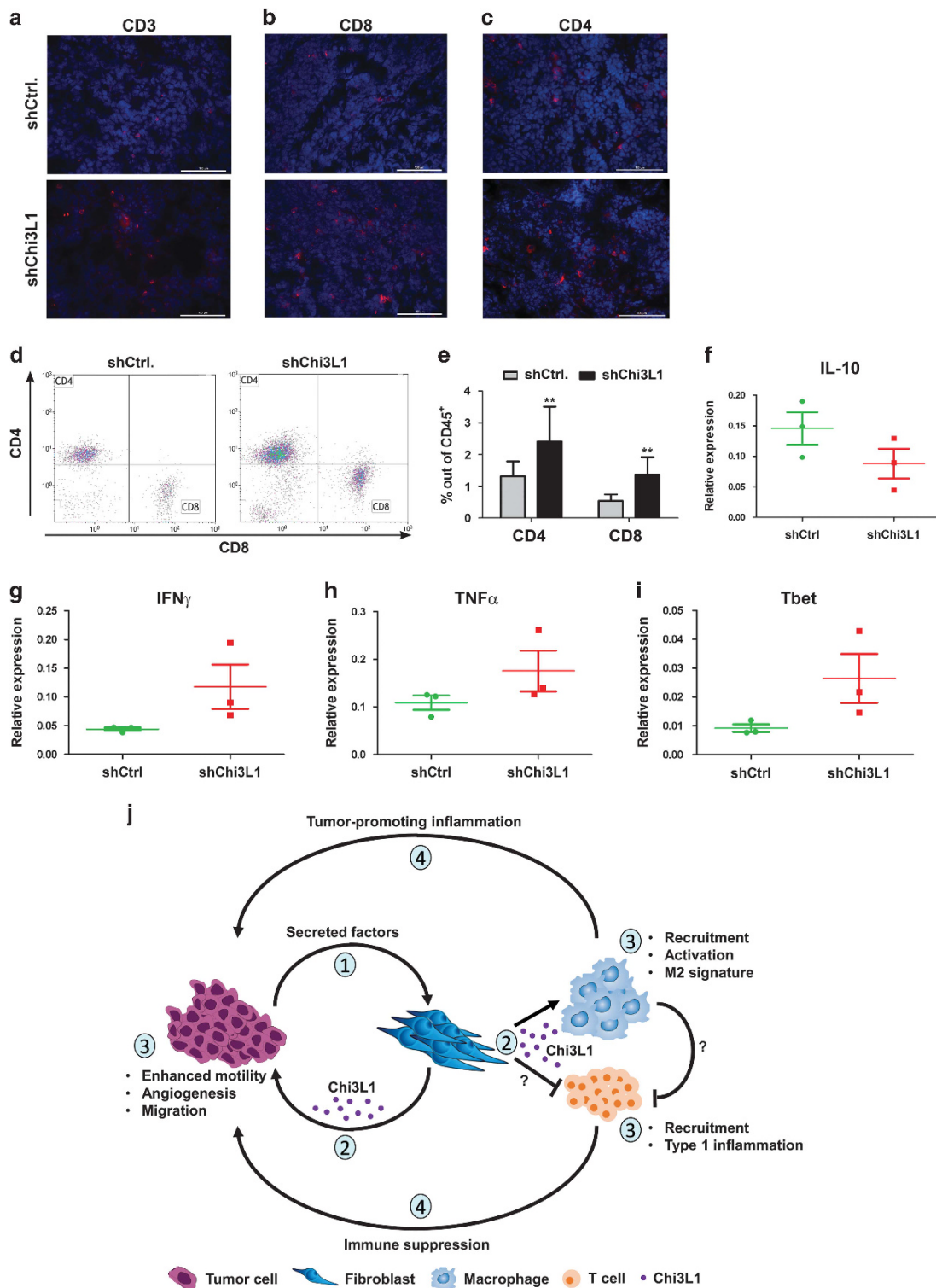


Figure 5. Fibroblast-derived Chi3L1 contributes to the formation of an immunosuppressed microenvironment. **(a–c)** Representative images of CD3 **(a)**, CD8 **(b)** and CD4 **(c)** staining of Met-1 tumors injected with shChi3L1 fibroblasts ($n=6$) or control fibroblasts ($n=3$). Multiple fields were analyzed from each group. Scale bar = 100 μ m. Magnification $\times 40$. **(d)** FACS analysis of CD4⁺ and CD8⁺ T cells (gated from CD45⁺CD3⁺) isolated from tumors. **(e)** Quantification of FACS analysis in **(d)**. Error bars represent s.d. $^{**}P < 0.01$, $n=3$ (shCtrl), $n=4$ (shChi3L1). **(f)** qRT-PCR analysis of IL-10 expression in mammary tumors injected with shChi3L1 fibroblasts vs control. Results are normalized to the housekeeping gene *Gapdh*. Error bars represent s.e.m., $n=3$ mice per group. **(g–i)** qRT-PCR analysis of Th1-related genes expression in mammary tumors injected with shChi3L1 fibroblasts vs control. Results are normalized to the housekeeping gene *Gapdh*. Error bars represent s.e.m., $n=3$ mice per group. **(j)** *Fibroblasts drive an immunosuppressive and growth-promoting microenvironment in breast cancer via secretion of Chi3L1*: Tumor-derived factors induce secretion of Chi3L1 from CAFs (1). CAF-derived Chi3L1 (2) supports tumor growth by direct effect on tumor cells, as well as by macrophages and T cells recruitment and reprogramming (3), resulting in enhancement of tumor promoting inflammation and immunosuppression (4).

cells, as we have demonstrated *in vitro*. However, our findings suggest that in addition, CAF-derived Chi3L1 reprograms tumor-associated macrophages to an M2-like phenotype, which is associated with tumor progression.⁴⁰

Fibroblasts and macrophages are key players in mediating tumor-promoting inflammation, but the functional relationship between these two cell populations, and its significance to tumor progression are poorly characterized.⁴⁵ We show that knockdown of Chi3L1 in fibroblasts attenuated M2-like differentiation of bone marrow-derived primary macrophages. Moreover, mammary tumors in which Chi3L1 was specifically knocked down in fibroblasts exhibited less M2-like macrophages, increased numbers of CD8⁺ T cells, and a shift of the CD4⁺ T cells towards a Th1 phenotype, suggesting that CAF-derived Chi3L1 is functionally important for driving an immunosuppressed tumor microenvironment. These results suggest that the previously demonstrated ability of CAFs to modulate an immunosuppressive microenvironment in tumors^{22,46,47} is mediated, at least partially, by their secretion of Chi3L1.

Notably, these pro-inflammatory and immunosuppressive effects of CAF-derived Chi3L1 were functionally important *in vivo*, as the effect of ablating Chi3L1 in fibroblasts had a profound effect on tumor growth and the immune cell milieu despite the continued secretion of Chi3L1 by cancer cells and macrophages, suggesting that stromal-derived factors, including Chi3L1, are required for immune modulation of the tumor microenvironment.

M2-like differentiation of macrophages and adaptive Th2 effector responses were shown to be aberrant in Chi3L1^{-/-} mice.²⁸ These findings are compatible with the demonstrated role of Chi3L1 in promoting lung fibrosis,⁴⁸ known to be associated with chronic Th2 inflammatory responses. Thus, it is conceivable that fibroblasts-derived Chi3L1 contributes to these pathologic phenotypes, but its distinct role was not previously determined. Our study suggests that in the tumor microenvironment, fibroblasts-derived Chi3L1 contributes to alternative differentiation of macrophages and to fostering of an immunosuppressive microenvironment, by affecting both TAMs and T cells.

Interestingly, we found that Chi3L1 was upregulated and secreted by lung fibroblasts isolated from MMTV-PyMT mice with pulmonary metastases, suggesting that CAF-derived Chi3L1 may have a functional role in the metastatic microenvironment. In agreement with this hypothesis, functional inhibition of Chi3L1 activity was shown to result in decreased lung metastases in a breast cancer model.⁴⁹ This inhibition of metastases formation was suggested to result from attenuating the activity of macrophage-derived Chi3L1, as expression of Chi3L1 in macrophages was linked with increased metastases.^{36,50} However, our findings imply that the effect of Chi3L1 inhibition on pulmonary metastasis of breast cancer may also result from targeting its secretion by metastases-associated fibroblasts. Future studies are required to better decipher the molecular mechanism by which stromal-derived Chi3L1 facilitates tumor metastasis.

In summary, this study deepens our understanding of the multifaceted interactions in the tumor microenvironment and demonstrates that CAF-derived Chi3L1 promotes tumor progression by complex interactions with tumor cells, macrophages and T cells that collectively enhance inflammation and tumor growth. Elucidating the molecular mechanisms by which CAFs and immune cells interact to mediate cancer-related inflammation in breast cancer will allow therapeutic manipulation of stromal molecular targets and provide a novel combinatorial approach to combat breast cancer progression, and to improve individualized therapeutic options.

MATERIALS AND METHODS

Mice

MMTV-PyMT mice were bred and maintained at the Tel Aviv University SPF facility. Normal FVB/n mice were obtained from negative littermates or purchased from Harlan, Israel. All experiments involving animals were approved by the TAU Institutional Animal Care and Use Committee. No statistical methods were used to predetermine sample size. The experiments were not randomized. The investigators were not blinded to allocation during experiments and outcome assessment.

Primary cells

NMFs and NLFs were isolated from mammary glands or lungs of 8–12 weeks old female FVB/n mice and cultured as previously described.²⁴ All experiments were performed with low passage (p2–4) fibroblasts. Multiple batches of fibroblasts were used.

Bone Marrow Macrophages (BMM) were prepared as previously described.⁵¹ BMM purity was confirmed by FACS analysis. All experiments were performed with passage 1 BMM. Multiple batches of BMM were used.

Cell lines

Met-1 mouse breast carcinoma cells were a kind gift from Dr Jeffrey Pollard. RAW 264.7 macrophages were a kind gift from Dr Tsaffir Zor. All cells were routinely tested for mycoplasma using the EZ-PCR mycoplasma test kit (Beit Haemek, Israel).

Conditioned media

Conditioned media was prepared as previously described.²⁴

Enzyme-Linked Immunosorbent Assay

Enzyme-Linked Immunosorbent Assay (ELISA) for Chi3L1 was performed using a commercial kit, according to manufacturer's protocol (R&D Systems; MC3L10). Fibroblasts were cultured with Met-1 CM for 24 h, washed and incubated with fresh SFM for additional 24 h. Media were collected, filtered with 0.45 µm filters and used for ELISA assays. Mouse sera were collected from normal FVB/n mice or MMTV-PyMT mice with advanced carcinoma.

Scratch assay

The assay was performed as previously described, with minor modifications.²⁴

Migration assay

Met-1 (5×10^4) or RAW 264.7 (1×10^5) cells were placed in the upper side of 24 Transwell inserts, with pore sizes of 8 µm, and incubated for 24 h in SFM or SFM supplemented with 100 ng/ml rChi3L1. Following incubation, the upper side of the apical chamber was fixed with methanol and stained with DAPI. Migrated cells were documented with a fluorescence microscope, and quantified with ImageJ software.

Western blotting

Lysates were prepared from cell pellets in RIPA lysis buffer. Protein determination was performed with Pierce BCA Protein Assay Kit. Cell extracts were resolved by SDS-PAGE and electroblotted onto nitrocellulose membranes (BioRad, Hercules, CA, USA). Membranes were probed with antibodies specific for ERK, AKT, p-ERK and p-Akt (Cell Signaling Technology, Danvers, MA, USA). Bands were visualized using ECL and quantified with ImageJ.

Quantitative real-time PCR

RNA isolation and qRT-PCR was performed as previously described.⁵² Expression results were normalized to GAPDH. Error bars represent s.d. of three technical repeats.

Methylene blue viability assay

The assay was performed as previously described.⁵³

XTT cell proliferation assay

The assay performed as previously described.²⁴

Orthotopic tumors

2×10^5 Met-1 cells and 6×10^5 shCtrl NMF or shChi3L1 NMF were injected into the right inguinal mammary gland of 8 weeks old FVB/n female mice and measured twice weekly with calipers until tumor growth reached a size of 15 mm in any diameter. Mice were killed and tumors were embedded in OCT or digested into single cell suspension for FACS analysis. Kaplan–Meier survival curve was calculated for mice that reached the endpoint of tumor growth.

FACS analysis

Mammary glands were isolated from mice. Single cell suspensions were prepared as we previously described.³⁰ Cells were stained using the following antibodies: F4/80-BV510, F4/80-APC, CD206-FITC, CD86-PE, CD4-APC/Cy7 (Biolegend, San Diego, CA, USA), CD11b-PerCP/Cy5.5, CD45-PE/Cy7, CD3-FITC, CD8a-APC (eBioscience, San Diego, CA, USA). DAPI was used to exclude dead cells (Molecular probes, Eugene, OR, USA; D3571). Analysis was performed with Gallios Flow Cytometer (Beckman Coulter, Nyon, Switzerland).

In vivo matrigel plug assay

2×10^5 Met-1 cells in 100 μ l PBS or PBS supplemented with 100 ng/ml rChi3L1 were mixed with 300 μ l Growth Factor Reduced Matrigel (Corning; 356231) and injected sub-cutaneous into 8-weeks-old FVB/n female mice. Two weeks after injection the plugs were dissected out and embedded in O.C.T (Tissue-Tek, Torrance, CA, USA) for histological analysis.

Immunostaining

Tissue preparation. Serial sections of 5–7 μ m were cut from fresh-frozen tissues that were embedded in OCT.

PicroSirius Red staining was performed as previously described.²⁴

Immunofluorescence. Tissue sections were incubated overnight at 4 °C with the following anti-mouse antibodies: CD3 (BioRad), α -SMA (Sigma-Aldrich, Rehovot, Israel), CD4 (Biolegend), CD8 (Novus, Littleton, CO, USA), F4/80 (AbD Serotec, Hercules, CA, USA) and Meca-32 (BD, San Jose, CA, USA). Secondary antibodies were purchased from Jackson ImmunoResearch Laboratories and applied for 1 h at room temperature. Sections were mounted with DAPI Fluoromount-G (Southern Biotech, Birmingham, AL, USA; 0100-20).

Microscopy, image capture and analysis

Images were taken with Leica DM4000B microscope and digital camera (Leica DFC 360FX), using the Leica Application Suite software. Brightness and contrast were adjusted equally in all images presented.

GEO data set analysis

Microarray data from Finak *et al.*³³ were analyzed for Chi3L1. Expression level is presented as the median expression in multiple breast cancer tissues from human invasive carcinomas in different grades or in normal breast tissue (Normal).

Statistical analysis

Data were analyzed using the Student *t* test, and considered significant when *P* value was ≤ 0.05 . All statistical tests were two-sided. Bar graphs represent the mean and s.d. across multiple independent experimental repeats. All experiments were performed at least twice, unless otherwise stated.

CONFLICT OF INTEREST

The authors declare no conflict of interest.

ACKNOWLEDGEMENTS

This research was supported by grants to NE from the European Research Council under the European Union's Horizon 2020 research and innovation programme

(grant agreement no. 637069 MetCAF), from the Israel Science Foundation (#813/12), the Israel Cancer Association and The Israel Cancer Research Fund (*Research Career Development Award*). We would like to thank Dr Yaron Carmi for scientific discussions, Shahar Biechonski and Hila Schwartz for their help with data analysis and helpful discussions, and Elad Yana for graphical assistance. We thank Dr Ariel Munitz for critical reading of the manuscript. This work was performed in partial fulfillment of the requirements for a PhD of Noam Cohen, Sackler School of Medicine, Tel Aviv University.

REFERENCES

- Mantovani A, Marchesi F, Porta C, Sica A, Allavena P. Inflammation and cancer: breast cancer as a prototype. *Breast* 2007; **16**: S27–S33.
- Colotta F, Allavena P, Sica A, Garlanda C, Mantovani A. Cancer-related inflammation, the seventh hallmark of cancer: links to genetic instability. *Carcinogenesis* 2009; **30**: 1073–1081.
- Hanahan D, Weinberg RA. Hallmarks of cancer: the next generation. *Cell* 2011; **144**: 646–674.
- Hanahan D, Coussens LM. Accessories to the crime: functions of cells recruited to the tumor microenvironment. *Cancer Cell* 2012; **21**: 309–322.
- de Visser KE, Eichten A, Coussens LM. Paradoxical roles of the immune system during cancer development. *Nat Rev Cancer* 2006; **6**: 24–37.
- DeNardo DG, Coussens LM. Inflammation and breast cancer. Balancing immune response: crosstalk between adaptive and innate immune cells during breast cancer progression. *Breast Cancer Res* 2007; **9**: 212.
- DeNardo DG, Barreto JB, Andreu P, Vazquez L, Tawfik D, Kolhatkar N *et al.* CD4(+) T cells regulate pulmonary metastasis of mammary carcinomas by enhancing protumor properties of macrophages. *Cancer Cell* 2009; **16**: 91–102.
- Lin EY, Pollard JW. Tumor-associated macrophages press the angiogenic switch in breast cancer. *Cancer Res* 2007; **67**: 5064–5066.
- Pollard JW. Tumour-educated macrophages promote tumour progression and metastasis. *Nat Rev Cancer* 2004; **4**: 71–78.
- Pollard JW. Macrophages define the invasive microenvironment in breast cancer. *J Leukocyte Biol* 2008; **84**: 623–630.
- Campbell MJ, Tonlaar NY, Garwood ER, Huo D, Moore DH, Khramtsov AI *et al.* Proliferating macrophages associated with high grade, hormone receptor negative breast cancer and poor clinical outcome. *Breast Cancer Res Treatment* 2010; **128**: 703–711.
- DeNardo DG, Brennan D, Rexhapaj E, Ruffell B, Shiao S, Gallagher WM *et al.* Leukocyte complexity in breast cancer predicts overall survival and functionally regulates response to chemotherapy. *Cancer Discov* 2011; **1**: 54–67.
- Noy R, Pollard JW. Tumor-associated macrophages: from mechanisms to therapy. *Immunity* 2014; **41**: 49–61.
- Qian BZ, Pollard JW. Macrophage diversity enhances tumor progression and metastasis. *Cell* 2010; **141**: 39–51.
- Doedens AL, Stockmann C, Rubinstein MP, Liao D, Zhang N, DeNardo DG *et al.* Macrophage expression of hypoxia-inducible factor-1 α suppresses T-cell function and promotes tumor progression. *Cancer Res* 2010; **70**: 7465–7475.
- Ruffell B, Chang-Strachan D, Chan V, Rosenbusch A, Ho CM, Pryer N *et al.* Macrophage IL-10 blocks CD8+ T cell-dependent responses to chemotherapy by suppressing IL-12 expression in intratumoral dendritic cells. *Cancer Cell* 2014; **26**: 623–637.
- Walker RA. The complexities of breast cancer desmoplasia. *Breast Cancer Res* 2001; **3**: 143–145.
- Kalluri R, Zeisberg M. Fibroblasts in cancer. *Nat Rev Cancer* 2006; **6**: 392–401.
- Ostman A, Augsten M. Cancer-associated fibroblasts and tumor growth—bystanders turning into key players. *Curr Opin Genet Dev* 2009; **19**: 67–73.
- Erez N, Glanz S, Raz Y, Avivi C, Barshack I. Cancer associated fibroblasts express pro-inflammatory factors in human breast and ovarian tumors. *Biochem Biophys Res Commun* 2013; **437**: 397–402.
- Erez N, Truitt M, Olson P, Arron ST, Hanahan D. Cancer-associated fibroblasts are activated in incipient neoplasia to orchestrate tumor-promoting inflammation in an NF- κ B-dependent manner. *Cancer Cell* 2010; **17**: 135–147.
- Feig C, Jones JO, Kraman M, Wells RJ, Deonarine A, Chan DS *et al.* Targeting CXCL12 from FAP-expressing carcinoma-associated fibroblasts synergizes with anti-PD-L1 immunotherapy in pancreatic cancer. *Proc Natl Acad Sci USA* 2013; **110**: 20212–20217.
- Martey CA, Pollock SJ, Turner CK, O'Reilly KM, Baglioni CJ, Phipps RP *et al.* Cigarette smoke induces cyclooxygenase-2 and microsomal prostaglandin E2 synthase in human lung fibroblasts: implications for lung inflammation and cancer. *Am J Physiol Lung Cell Mol Physiol* 2004; **287**: L981–L991.
- Sharon Y, Raz Y, Cohen N, Ben-Shmuel A, Schwartz H, Geiger T *et al.* Tumor-derived Osteopontin reprograms normal mammary fibroblasts to promote inflammation and tumor growth in breast cancer. *Cancer Res* 2015; **75**: 963–973.

- 25 Lotti F, Jarrar AM, Pai RK, Hitomi M, Lathia J, Mace A et al. Chemotherapy activates cancer-associated fibroblasts to maintain colorectal cancer-initiating cells by IL-17A. *J Exp Med* 2013; **210**: 2851–2872.
- 26 Lee CG, Da Silva CA, Dela Cruz CS, Ahangari F, Ma B, Kang MJ et al. Role of chitin and chitinase/chitinase-like proteins in inflammation, tissue remodeling, and injury. *Ann Rev Physiol* 2011; **73**: 479–501.
- 27 Eurich K, Segawa M, Toei-Shimizu S, Mizoguchi E. Potential role of chitinase 3-like-1 in inflammation-associated carcinogenic changes of epithelial cells. *World J Gastroenterol* 2009; **15**: 5249–5259.
- 28 Lee CG, Hartl D, Lee GR, Koller B, Matsuura H, Da Silva CA et al. Role of breast regression protein 39 (BRP-39)/chitinase 3-like-1 in Th2 and IL-13-induced tissue responses and apoptosis. *J Exp Med* 2009; **206**: 1149–1166.
- 29 Bigg HF, Wait R, Rowan AD, Cawston TE. The mammalian chitinase-like lectin, YKL-40, binds specifically to type I collagen and modulates the rate of type I collagen fibril formation. *J Biol Chem* 2006; **281**: 21082–21095.
- 30 Sharon Y, Alon L, Glanz S, Servais C, Erez N. Isolation of normal and cancer-associated fibroblasts from fresh tissues by fluorescence activated cell sorting (FACS). *J Vis Exp* 2013. e4425.
- 31 Lin EY, Jones JG, Li P, Zhu L, Whitney KD, Muller WJ et al. Progression to malignancy in the polyoma middle T oncoprotein mouse breast cancer model provides a reliable model for human diseases. *Am J Pathol* 2003; **163**: 2113–2126.
- 32 Libreros S, Garcia-Areas R, Keating P, Carrio R, Iragavarapu-Charyulu VL. Exploring the role of CHI3L1 in 'pre-metastatic' lungs of mammary tumor-bearing mice. *Front Physiol* 2013; **4**: 392.
- 33 Finak G, Bertos N, Pepin F, Sadekova S, Souleimanova M, Zhao H et al. Stromal gene expression predicts clinical outcome in breast cancer. *Nat Med* 2008; **14**: 518–527.
- 34 Borowsky AD, Namba R, Young LJ, Hunter KW, Hodgson JG, Tepper CG et al. Syngeneic mouse mammary carcinoma cell lines: two closely related cell lines with divergent metastatic behavior. *Clin Exp Metastasis* 2005; **22**: 47–59.
- 35 Shao R, Hamel K, Petersen L, Cao QJ, Arenas RB, Bigelow C et al. YKL-40, a secreted glycoprotein, promotes tumor angiogenesis. *Oncogene* 2009; **28**: 4456–4468.
- 36 Libreros S, Garcia-Areas R, Iragavarapu-Charyulu V. CHI3L1 plays a role in cancer through enhanced production of pro-inflammatory/pro-tumorigenic and angiogenic factors. *Immunol Res* 2013; **57**: 99–105.
- 37 Qian BZ, Li J, Zhang H, Kitamura T, Zhang J, Campion LR et al. CCL2 recruits inflammatory monocytes to facilitate breast-tumour metastasis. *Nature* 2011; **475**: 222–225.
- 38 Murray PJ, Allen JE, Biswas SK, Fisher EA, Gilroy DW, Goerdts S et al. Macrophage activation and polarization: nomenclature and experimental guidelines. *Immunity* 2014; **41**: 14–20.
- 39 Mantovani A, Sica A. Macrophages, innate immunity and cancer: balance, tolerance, and diversity. *Curr Opin Immunol* 2010; **22**: 231–237.
- 40 Sica A, Mantovani A. Macrophage plasticity and polarization: *in vivo* veritas. *J Clin Invest* 2012; **122**: 787–795.
- 41 Ali HR, Provenzano E, Dawson SJ, Blows FM, Liu B, Shah M et al. Association between CD8+ T-cell infiltration and breast cancer survival in 12,439 patients. *Ann Oncol* 2014; **25**: 1536–1543.
- 42 Kawada M, Seno H, Kanda K, Nakanishi Y, Akitake R, Komekado H et al. Chitinase 3-like 1 promotes macrophage recruitment and angiogenesis in colorectal cancer. *Oncogene* 2012; **31**: 3111–3123.
- 43 Jensen BV, Johansen JS, Price PA. High levels of serum HER-2/neu and YKL-40 independently reflect aggressiveness of metastatic breast cancer. *Clin Cancer Res: Off J Am Assoc Cancer Res* 2003; **9**: 4423–4434.
- 44 Johansen JS, Christensen IJ, Riisbro R, Greenall M, Han C, Price PA et al. High serum YKL-40 levels in patients with primary breast cancer is related to short recurrence free survival. *Breast Cancer Res Treat* 2003; **80**: 15–21.
- 45 Komohara Y, Takeya M. CAFs and TAMs: maestros of the tumour microenvironment. *J Pathol* 2016; **241**: 313–315.
- 46 Liao D, Luo Y, Markowitz D, Xiang R, Reisfeld RA. Cancer associated fibroblasts promote tumor growth and metastasis by modulating the tumor immune microenvironment in a 4T1 murine breast cancer model. *PLoS One* 2009; **4**: e7965.
- 47 Servais C, Erez N. From sentinel cells to inflammatory culprits: cancer-associated fibroblasts in tumour-related inflammation. *J Pathol* 2013; **229**: 198–207.
- 48 Zhou Y, Peng H, Sun H, Peng X, Tang C, Gan Y et al. Chitinase 3-like 1 suppresses injury and promotes fibroproliferative responses in Mammalian lung fibrosis. *Sci Transl Med* 2014; **6**: 240ra76.
- 49 Libreros S, Garcia-Areas R, Shibata Y, Carrio R, Torroella-Kouri M, Iragavarapu-Charyulu V. Induction of proinflammatory mediators by CHI3L1 is reduced by chitin treatment: decreased tumor metastasis in a breast cancer model. *Int J Cancer* 2012; **131**: 377–386.
- 50 Ma B, Herzog EL, Lee CG, Peng X, Lee CM, Chen X et al. Role of Chitinase 3-like-1 and Semaphorin 7a in pulmonary melanoma metastasis. *Cancer Res* 2014; **75**: 487–496.
- 51 Karo-Atar D, Itan M, Pasmanik-Chor M, Munitz A. MicroRNA profiling reveals opposing expression patterns for miR-511 in alternatively and classically activated macrophages. *J Asthma: Off J Assoc Care Asthma* 2015; **52**: 545–553.
- 52 Schwartz H, Blacher E, Amer M, Livneh N, Abramovitz L, Klein A et al. Incipient melanoma brain metastases instigate astrogliosis and neuroinflammation. *Cancer Res* 2016; **76**: 4359–4371.
- 53 Mizrachi-Schwartz S, Kravchenko-Balasha N, Ben-Bassat H, Klein S, Levitzki A. Optimization of energy-consuming pathways towards rapid growth in HPV-transformed cells. *PLoS ONE* 2007; **2**: e628.



This work is licensed under a Creative Commons Attribution-NonCommercial-NoDerivs 4.0 International License. The images or other third party material in this article are included in the article's Creative Commons license, unless indicated otherwise in the credit line; if the material is not included under the Creative Commons license, users will need to obtain permission from the license holder to reproduce the material. To view a copy of this license, visit <http://creativecommons.org/licenses/by-nc-nd/4.0/>

© The Author(s) 2017

Supplementary Information accompanies this paper on the Oncogene website (<http://www.nature.com/onc>)